Sigma Journal of Engineering and Natural Sciences
Web page info: https://sigma.yildiz.edu.tr
DOI: 10.14744/sigma.2022.00079

Research Article

The relationship between mucilage covered areas and chlorophyll-a concentration: The sea of Marmara case

Ahmet Batuhan POLAT[1]*, Fusun BALIK SANLI[2], Ozgun AKCAY[1]

[1]*Canakkale Onsekiz Mart University, Faculty of Engineering, Geomatics Engineering, Canakkale 17020, Türkiye*
[2]*Yildiz Technical University, Faculty of Civil Engineering, Geomatics Engineering, Istanbul 34220, Türkiye*

ARTICLE INFO

Article history
Received: 23 August 2021
Accepted: 18 October 2021

Key words:
Sentinel-2; Optical Images; Sea Monitoring; Organic Matter

ABSTRACT

Today, mucilage, or as it is known by the people, sea saliva, which directly affects the natural life and trade opportunities of the Marmara Sea, has more and more serious consequences day by day. The rapid detection of the spreading areas of the mucilage is of great importance for the cleaning works to be carried out. Remote sensing satellites have the great advantage of detecting the mucilage layer on the sea surface and studying its propagation. It has an important place in monitoring the change in that region over time and associating it with other ecological analysis, especially thanks to the ability to take images from the same region with frequent repetitions. Within the scope of this study, the mucilage distribution areas on the sea surface in the Dardanelles Strait, Gemlik Bay and Izmit Bay were investigated temporally and the concentration of chlorophyll-a, which is the main component organic matter of phytoplankton, and it is also the main cause of mucilage in the sea, was investigated and associated with mucilage areas. The satellite images used in the study were obtained from the Sentinel-2 multispectral optical satellite and the areas were determined by interpreting the images before and after mucilage propagation. Normalized Water Index (NDWI), a band index, was used to determine the mucilage area. As a result of the analysis, the mucilage rates in the sea were determined from the images on the dates used in the study. These rates were found as approximately 2.03% in the Dardanelles Strait, approximately 6.80% and 3.52% in the Gulf of Gemlik, where satellite images were examined at 10-day intervals, and approximately 7.44% in the Gulf of Izmit. When we look at the increase in the chlorophyll-a concentration in the sea for the same regions and dates, it is detected as about 0.84% in the Dardanelles Strait, 272.64% and 84.06% in the Gulf of Gemlik, and 8.22% in the Gulf of Izmit. When we look at the results, it is understood that the chlorophyll-a concentration and the spread of the mucilage layer are related to each other. In the light of these results, it is expected that using remote sensing techniques can be easily used for detecting mucilage, which is formed on the sea surface and spreads over large areas, and be a preliminary analysis study for rapid interventions.

Cite this article as: Polat AB, Balık Sanli F, Akcay O. The relationship between mucilage covered areas and chlorophyll-a concentration: The sea of Marmara case. Sigma J Eng Nat Sci 2022;40(3):673–684.

***Corresponding author.**
*E-mail address: abpolat@comu.edu.tr

This paper was recommended for publication in revised form by Ahmet Selim Dalkılıç

INTRODUCTION

Life below water, which is the 14th article of the Sustainable Development Goals (SDGs), which came into force in 2016 by the United Nations and covers the goals until 2030, aims to protect the biodiversity in the seas and oceans and to use these resources sustainably [1]. For Turkey, which is surrounded by seas on three sides due to its geographical location, the lack of protection of marine areas may lead to the destruction of the marine ecosystem that may be encountered in the future and the loss of commercial activities. In the fishery utilization statistics released by the Turkish Statistics Agency, the marine fish catch in 2020 is determined to be 291,000 tons and 910 tons [2]. In a sea area with such a wide range of fisheries, seawater pollution must be kept to a minimum in order to protect the diversity of fish.

The Sea of Marmara is an inland sea with a total of six coasts, namely Istanbul, Tekirdağ, Çanakkale, Kocaeli, Yalova and Bursa. Besides fishing activities, it has a strategically important maritime traffic route because it connects the Mediterranean and the Black Sea [3]. Since the Sea of Marmara is a region with intense maritime traffic, oil and other wastes leaking from ships cause a high level of sea pollution problems [4]. In the Sea of Marmara, which is on an important sea transit route, there are substances that affect the number of bacteria in the sea in the ballast water that many ships coming from various ports leave directly into the sea [5]. Another major factor in marine pollution is the large heavy industrial zones in the Marmara Sea basin. Most of these industrial zones release their wastes directly into seawater without any treatment [6]. In addition, the direct meeting of the currents from the Black Sea and the Mediterranean Sea in the Marmara Sea causes the proliferation of pollutants in this inland sea [7,8].

Harmful phytoplankton poses a major problem for the sustainable development of sea coasts and interior areas [9]. Lancelot determined in his study that every spring, Phaeocystis which is a phytoplankton species, creates a large algal bloom due to disruptions in the food chain and covers the entire North Sea coast [10]. The mucilage formed as a result of this algal bloom has been stated as the accumulation of certain climatic conditions and organic matter [11,12]. Marine mucilage, also called sea snow, causes small-sized organisms to attach to each other when suitable temperature conditions occur, and as a result, spread over very large areas with a nebula image [13]. Mucilage, which is scientifically known as algae bloom, leads organic matter accumulation faster than it should be, reduces oxygen level in the sea and causes substantial damage to the marine bio system. Owing to its rapid spread and wide coverage, mucilage can greatly affect marine ecosystems, fisheries, and tourism [14]. The intensification of mucilage formation depending on climatic conditions and sea temperature has been shown in certain studies in the literature [15–17].

In the Sea of Marmara, an algae explosion occurred recently in 2007, and most of the sea surface is covered with mucilage. In the study of Tüfekçi, the mucilage content of the samples collected from the Gulf of Izmit was examined and it was determined that the structure was formed as a result of 3 different phytoplankton species [18]. Artüz's report in 2007, in which he examined the mucilage spread and its causes as a result of the algae explosion in the Marmara Sea, showed that the accumulated mucilage did not disappear with the change in water temperature, but only changed its form [19]. In this way, he stated in his report that it cannot be said that the effect is completely over and that the problems will increase in the future. In the study conducted by Keleş et al. in 2020, the negative effects of the mucilage covering the Marmara Sea and affecting the marine ecosystem in 2007 on the fishing sector were examined and it was shown that the fishery incomes decreased greatly [20].

Remote sensing is critical for the continuous monitoring and protection of the environment, as it provides rapid, repeated observations, coverage of large areas, and continuous imaging [21]. In terms of environmental analysis, agricultural developments, urban land development, deforestation, and hydrological analysis can be cited as areas of use for remote sensing [22–24]. As for the marine and ocean pollution, remote sensing technologies allow real-time monitoring of oil and chemical spills, high algal blooms, and many other pollutants on the water surface [25]. In the literature, it has been shown in many studies that optical and radar satellites are used to detect chemical leaks, especially from ships to the open seas and in ports [26–29]. In order to determine the water quality according to the color scale of seawater, different parameters such as chlorophyll-a concentration, total suspended matter, turbidity are examined according to the reflection values of optical satellite images in water [30–33]. There are studies with remote sensing methods for the marine mucilage problem in the Sea of Marmara in 2021. Acar et al. demonstrated the fast detectability of mucilage areas with the Google Earth Engine and determined the mucilage areas instantly with high accuracy [34]. Again, in the study of Kavzoğlu et al., pixel and object-based classification methods were used while determining the mucilage areas, and it was determined that the object-based classification method gave a higher accuracy result [35].

Chlorophyll-a concentration is one of the most common parameters for evaluating phytoplankton dynamics and carbon cycle events for mucilage detection [36,37]. Chlorophyll-a concentration, which is the main pigment of harmful phytoplankton, and is also known as algal blooms and causes mucilage, is a parameter that shows the trophic state of water [38–40]. The important point is that chlorophyll-a level does not provide sufficient information for mucilage detection. The direct cause of mucilage is not

chlorophyll-a. The presence of chlorophyll-a in water may be due to many different factors. Studies added to the literature have shown that parameters determining the rate of water pollution such as chlorophyll-a may increase in shallow coasts under different conditions [41]. It is also used as an important parameter in the determination of algal blooms, water clarity and in-water nutrient concentrations [41]. Chlorophyll-a concentration has been used in many studies and added to the literature for the examination and analysis of water quality with optical satellite images. Watanabe et al., carried out a study using Landsat-8 satellite images, and observed the increase of phytoplankton, which is organic matter, depending on the chlorophyll-a concentration in man-made water reservoirs, and modeled the trophic image [42]. Since spectral band values are used to observe the chlorophyll-a concentration, studies have also been carried out with different optical satellites. For example, in a study conducted by Augusto-Silva et al. in 2014, the images of the European Space Agency's MERIS satellite, whose mission was terminated in 2012, and the Normalized Chlorophyll Index (NDCI), an image analysis index of chlorophyll-a concentration values according to image reflection values, were compared [43]. Its usability in the detection of organic matter in reservoirs has been investigated.

Within the scope of the study, the Sentinel-2 an optical satellite of the European Space Agency, was used. Detailed information about the satellite is given in the method section. When water quality analysis is performed with the help of Sentinel-2 chlorophyll a concentration, it can work in micro-regions due to its high spatial resolution of up to 10 meters [44]. The Sentinel-2 satellite is not designed for remote sensing directly on the water surface, but it provides sufficient resolution to distinguish water bodies from land [45].

The purpose of this research is to use Sentinel-2 optical satellite imagery to determine the area of mucilage on the sea surface and determine the area they cover. The Normalized Water Index (NDWI), which was obtained from different band values of the satellite image, was used to separate the water surface from the mucilage, and thus the temporal spread of the mucilage in the determined study areas was determined. In addition, the chlorophyll-a concentration calculation was carried out for different dates with the help of optical satellite images taken from the sea, and the relationship between the formation and spread of mucilage in the Sea of Marmara, which is considered as an algae explosion, and the chlorophyll-a concentration in the seawater was examined. Thus, the mucilage problem, which is a big problem for the ecology of the Marmara Sea and the trade route, is aimed to be a preliminary analysis for the local cleaning studies to be carried out in the regions where the mucilage layer is concentrated by quickly detecting the regions with high spread with remote sensing methods.

STUDY AREA AND DATA

The study area samples were chosen on the Dardanelles Strait, Gemlik Bay, and Izmit Bay. The mucilage was first

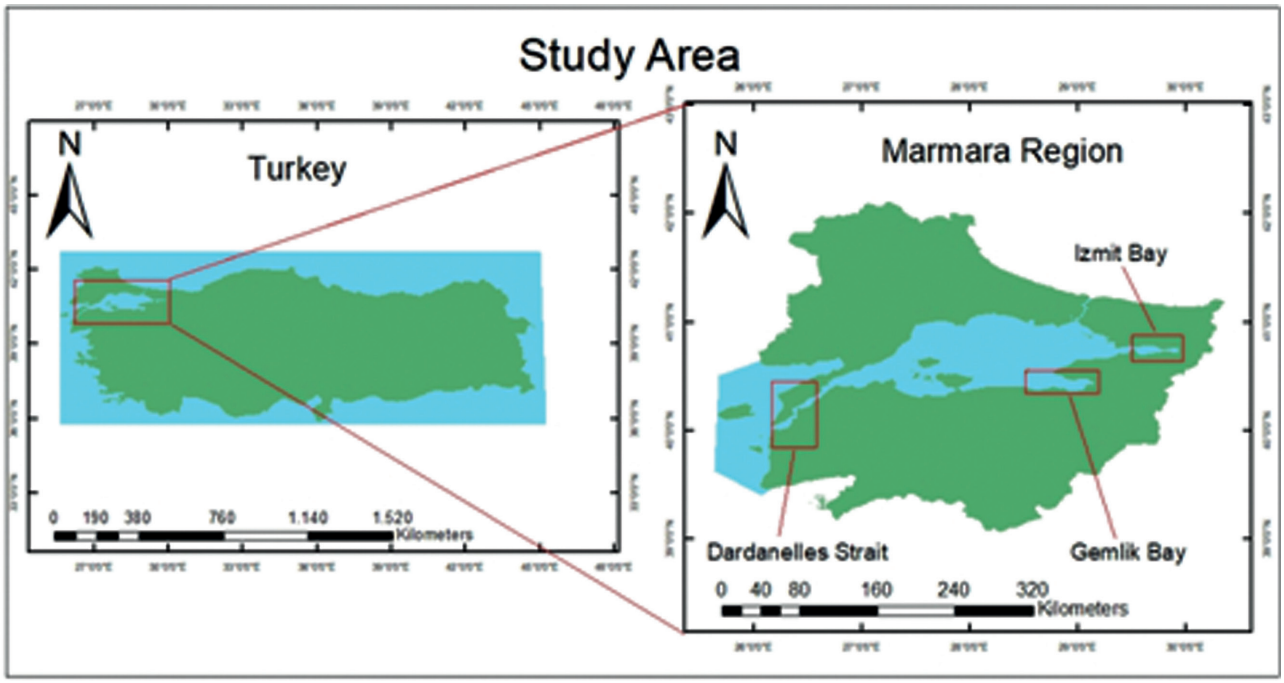

Figure 1. Study area.

Table 1. Sentinel-2 satellite image properties

Bands	Central wavelengths(μm)	Wave width(nm)	Spatial resolution (m)
Band 1 – Coastal Aerosol	0.443	20	60
Band 2 – Blue	0.490	65	10
Band 3 – Green	0.560	35	10
Band 4 – Red	0.665	30	10
Band 5 – Vegetation Red Edge	0.705	15	20
Band 6 - Vegetation Red Edge	0.740	15	20
Band 7 - Vegetation Red Edge	0.783	20	20
Band 8 – Near-Infrared (NIR)	0.842	115	10
Band 8A - Vegetation Red Edge	0.865	20	20
Band 9 – Water Vapour	0.945	20	60
Band 10 -Shortwave Infrared (SWIR)- Cirrus	1.375	30	60
Band 11 - Shortwave Infrared (SWIR)	1.610	90	20
Band 12 - Shortwave Infrared (SWIR)	2.190	180	20

Table 2. Image acquisition dates

Image No	Study area	Sentinel 2 Image Acquisition dates	Mucilage Observation Status
1	Dardanelles Strait	3 March 2021	Before
2	Dardanelles Strait	12 April 2021	Present
3	İzmit Bay	1 September 2020	Before
4	İzmit Bay	19 May 2021	Present
5	Gemlik Bay	11 October 2020	Before
6	Gemlik Bay	9 May 2021	Present
7	Gemlik Bay	19 May 2021	Present

seen in Dardanelles Strait in the Sea of Marmara in early April 2021, then seen in Gemlik Bay and Izmit Bay on the coasts of Bursa in May 2021 where mucilage covered a large area. In Figure 1, the locations of the study areas where satellite images were taken are shown on the map.

The optical satellite image used was obtained from the Sentinel-2 constellation satellite images launched into its orbit as part of the European Space Agency's Copernicus program. The Sentinel-2 satellite is an optical satellite launched into orbit in 2014. Sentinel-2 is a multi-band satellite system with 13 spectral bands. The spatial resolution of the bands varies between 10 m and 60 m, and it has a coverage area of 290 km. Thanks to the Sentinel 2a and Sentinel 2b constellations, the same region can be imaged every five days [46]. The advantage of the Sentinel-2 optical satellite over the optical satellites launched into orbit in previous years is that it offers a higher spatial resolution and has more spectral bands [47]. In Table 1, the technical specifications of the images taken from the Sentinel-2 satellite are given.

In the scope of the study, a total of 7 optical satellite images were used for three different regions. Three of the optical images used were obtained before the spread of the mucilage layer to the regions, while the remaining four images were obtained after the mucilage layer spread over the sea. Image acquisition dates are given in Table 2.

The reason for the differences between the pre-and post-event acquisition dates is that optical satellite images are affected by weather conditions. Since factors such as cloud ratio affect the visibility of clear places in the satellite image, image acquisitions were carried out on the dates when the most suitable conditions were created in different study areas. For this reason, 2 satellite images are available for the Dardanelles Strait and İzmit Bay, on the other hand 3 satellite images are available in the Gemlik Bay. The reason for the differences in the number of satellite images is the absence of satellite imagery under suitable conditions on the days when there is a mucilage layer on the sea surface in both study regions. The first image was chosen when no mucus formation was observed on the sea surface, and

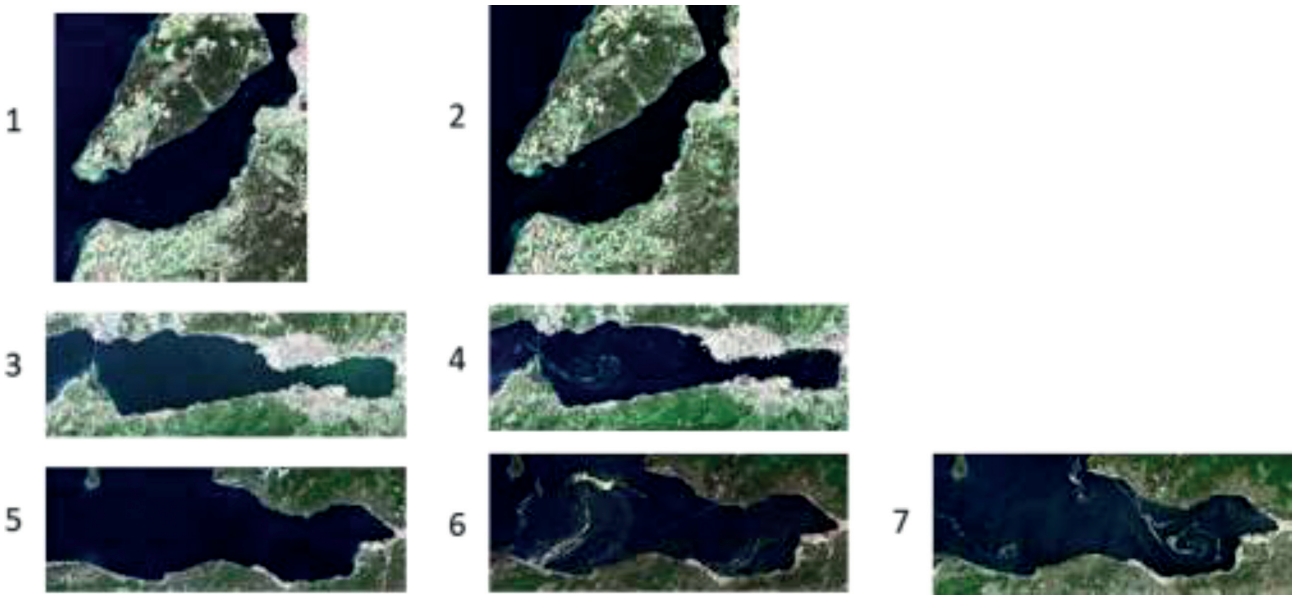

Figure 2. Sentinel-2 optical satellite images used in the study.

the second image was chosen after the mucus was spread on the sea surface. The satellite image provided is shown in Figure 2, with visible band composition.

METHODOLOGY

In order to perform the study, first it is necessary to collect available cloudless satellite images for the defined study areas. Then the satellite images need to composed by using different band combinations to determine the spreading areas of the mucilage. Next, the chlorophyll-a concentration in the optical images of the same date is calculated in order to monitor the organic matter ratio in the regions where the mucilage areas are concentrated. Finally, the correlation between chlorophyll-a concentration and the spread of mucilage areas are examined and interpreted. Figure 3 shows the workflow in the study.

DETECTION OF MUCILAGE AREAS

Normalized Water Index (NDWI) images were obtained by using the combination of optical satellite image bands to detect mucilage areas formed on the sea surface. The NDWI was first developed by McFeeters in 1996 to identify bodies of water. McFeeters (1996) found that NDWI takes advantage of reflected near infrared and green light in the visible region while removing terrestrial features and vegetation [48]. NDWI is one of the most suitable methods for detecting water bodies by remote sensing [49]. This is because NDWI obtained from remote sensing data is very sensitive to the change in hydrological conditions [50]. The NDWI formula is as follows [48];

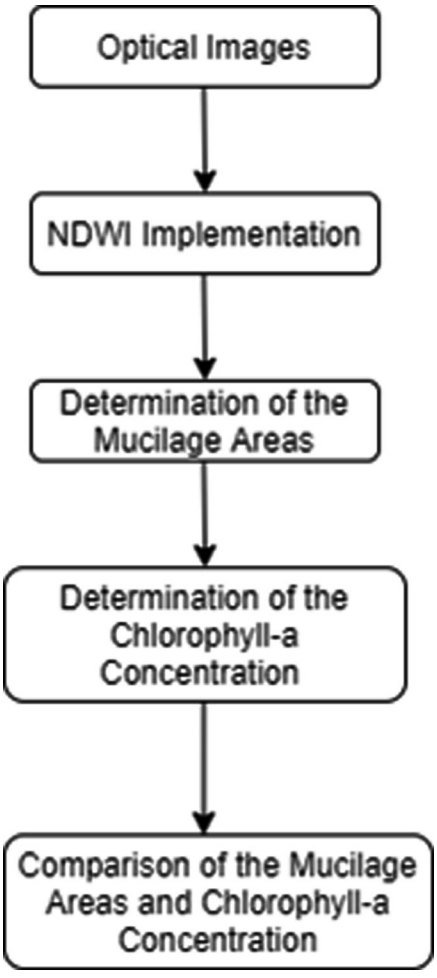

Figure 3. Workflow of the study.

$$NDWI = \frac{Green\ Band - Near - Infrared(NIR)\ Band}{Green\ Band + Near - Infrared(NIR)\ Band} \quad (1)$$

In the study, visible (VIS) and infrared (IR) bands of Sentinel-2 satellite images were used. The Green Band corresponds to Band 3 with a center wavelength of 0.560 μm, while the Near Infrared (NIR) band corresponds to Band 8 with a center wavelength of 0.842 μm. The reason for using these bands when identifying water areas is that NIR achieves minimal reflection from water surfaces while achieving a high level of reflection in non-water areas [51]. It is also desired to maximize the reflection of the water surface by using the green band. The first procedure to detect the mucilage area is to use the NDWI value to detect the sea surface from a satellite image taken before the mucilage spreads to the surface of the sea. Then, the sea areas were determined again by using the satellite images and NDWI values gathered after the mucilage spread over the sea surface. The differences between the sea areas obtained before and after the mucilage spread on the sea were calculated, thus the mucilage area on the surface was obtained. In addition, the mean NDWI values for each image were calculated, and the mean value changes before and after mucilage were compared. While NDWI values were calculated, band combinations were obtained with ArcGIS software.

CALCULATION OF CHLOROPHYLL-A CONCENTRATION IN STUDY AREAS

Chlorophyll-a concentration was calculated in order to calculate the time-dependent variation of the amount of organic matter on the sea surface and to correlate before and after the dissemination of mucilage on the sea surface. The increase in the concentration of chlorophyll-a leads to organic load and organic waste precipitation in the water deeper, resulting in the fragmentation of bacteria and the reduction of oxygen in the water, and the lack of oxygen in the marine ecology [52].

In order to determine chlorophyll-a by remote sensing method, the relationships between narrowly spaced bands or reflections in band ratios and chlorophyll-a are examined [53]. The algorithms based on the relationship between chlorophyll-a and the regions in the visible part of the spectrum referred to as the "red edge", show a correlation between the reflection difference between the near-infrared and the red region [54]. These spectral regions are suitable ranges for determining the concentration of chlorophyll-a, even in water with a high percentage of dissolved substances [55].

In this study, the Sentinel-2 satellite was used to detect chlorophyll-a concentration, which can be detected in in a very narrow range of electromagnetic spectrum, due to its multi-spectral feature. The Sentinel-2 bands closest to the ranges in which the chlorophyll-a concentration is optimally detected are Band 4 - Red with a central wavelength of 0.665 μm and Band 5 - Vegetation red edge with a central wavelength of 0.705 μm, respectively. Chlorophyll-a concentration was calculated for before and after mucilage spread in the study areas, and the average concentration values were recorded in micrograms/L (mgm^{-3}). Finally, after calculating the chlorophyll-a concentrations in the study areas, their compatibility with the mucilage areas extracted using NDWI and the relationship between them were examined.

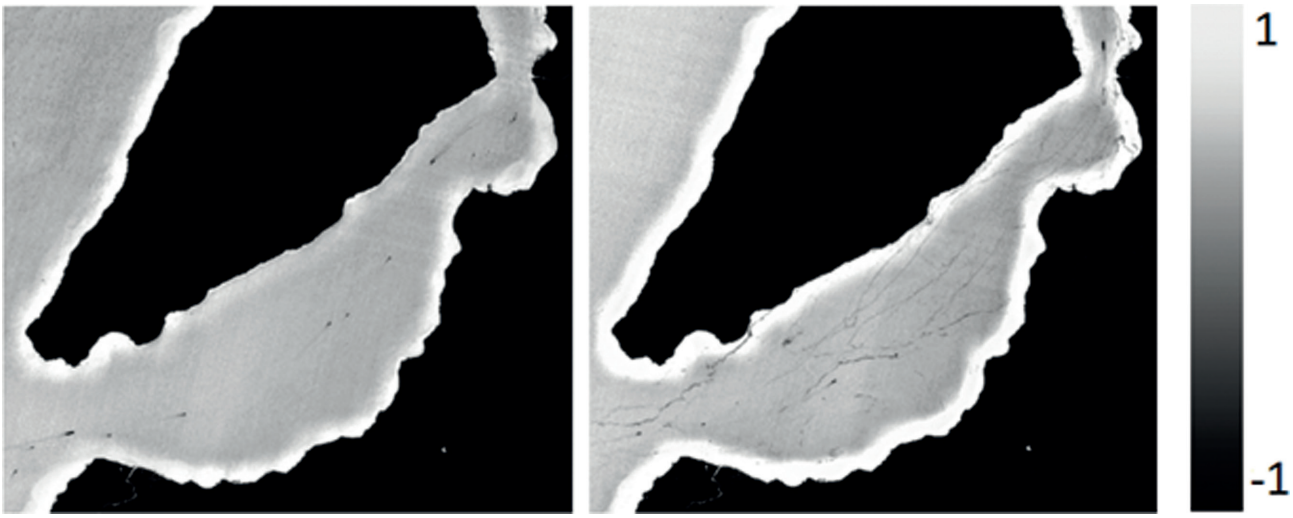

Figure 3. Dardanelles Strait - NDWI map (The image on the left is before mucilage, and the image on the right is the presence of mucilage).

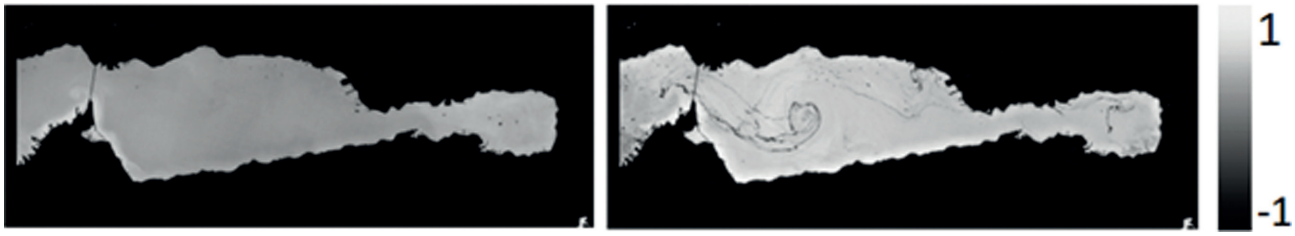

Figure 4. Izmit Bay - NDWI map (The image on the left is before mucilage, and the image on the right is the presence of mucilage).

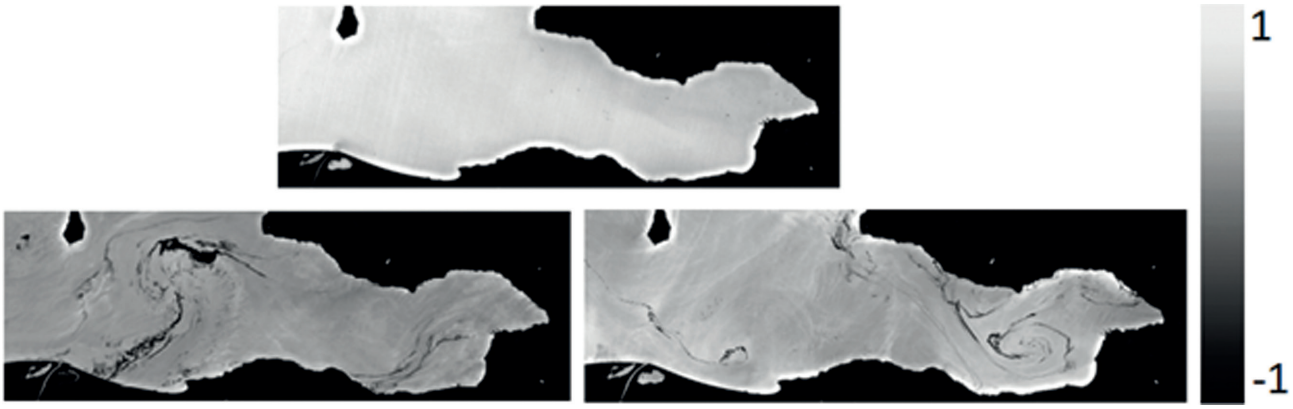

Figure 5. Gemlik Bay – NDWI map (The image above is before mucilage, and the images below shows the presence of mucilage ten days apart).

RESULTS AND DISCUSSION

First of all, NDWI images were obtained by using satellite images taken before and after the mucilage propagates at the sea. The mucilage coverage was determined and plotted from the NDWI images (Figure 3, Figure 4, and Figure 5). The color scale next to the figures shows the intensity of the NDWI reflection values. A low NDWI values are close to -1, while 1 indicates high NDWI values. On the other hand, reflections close to -1 are shown in black, while reflections close to 1 are shown in white.

The mucilage area of the study area is obtained by subtracting the difference between the sea area pre and after the event. The percentage of change is the ratio of these areas to each other. In addition, the average NDWI values in the satellite images were calculated and the differences were examined. Average NDWI values are the mean of the total NDWI values of all pixels in an image. As the mucilage areas increases, the mean NDWI value is expected to decrease. In Table 3, the mucilage area, the percentage of mucilage area, and the average NDWI value of all study areas are calculated and displayed.

When we look at the results in Table 3, it is seen that the mucilage spread on the sea surface is compatible with the NDWI maps. Considering the acquisition dates of the satellite images, a 421.59 m^2 mucilage formation was observed in the Dardanelles Strait between March 3 (Image 1) and April 12 (Image 2), 2021. It was observed that the mucilage formed on the sea surface on May 19 (Image 4), 2021 in the Gulf of Izmit covers an area of 1866.50 m^2. In the Gulf of Gemlik, a mucilage spread of 5874.44 m^2 is seen in the satellite image gathered on May 9 (Image 6), 2021, and of 2937.59 m^2 in the satellite image gathered on May 19

Table 3. Mucilage areas and mean NDWI values for all study areas

Image Number	Sea Area (m^2)	Mucilage Area (m^2)	Mucilage Area Change Percentage (%)	Average NDWI values
1	20720,73	–	–	0,0367
2	20299,14	421,59	2,03	0,0009
3	25102,12	–	–	0,2188
4	23235,62	1866,50	7,44	0,1850
5	86366,43	–	–	0,2629
6	80491,99	5874,44	6,80	0,0013
7	83428,84	2937,59	3,52	0,1090

(Image 7), 2021. It was observed that there was a decrease in mucilage areas in the Gemlik Bay within a 10-day period. When we look at the changes in the mucilage area as a percentage and the dates of the image acquisition are taken into account, it is observed that approximately 7.44% of the sea surface in the Gulf of Izmit is covered with mucilage. Also the highest mucilage coverage value is the on May 9, 2021. It was observed that mucilage coverage of the sea surface was approximately 6,80% in the Gulf of Gemlik.

As we examined the average NDWI values in the satellite images, the satellite images gathered before the mucilage propagation started in the Marmara Sea and the average NDWI values in the satellite images acquired after the mucilage propagation took place were compared. The average NDWI value, which was calculated as 0.0367 before mucilage formation in satellite images taken from the Dardanelles (Image 1-2), was calculated as 0.0009 after mucilage spread. On the other hand, in the satellite images showing the Gulf of Izmit (Image 3-4), the average NDWI value, which was calculated as 0.2188 before mucilage formation, was calculated as 0.1850 after the mucilage spread. Finally, when looking at the satellite images taken from the Gemlik Bay (Image 5-6-7), the average NDWI values calculated before the mucilage spread was calculated as 0.2629, while it was calculated as 0.0013 in the satellite image dated May 9, 2021, where the most mucilage area was detected. In the satellite image taken on May 19, 2021, where less mucilage area was detected than on May 9, 2021, the average NDWI values were calculated as 0.1090.

When we examine the mean chlorophyll-a concentrations in the sea areas before and after the mucilage spread, the value calculated as 0.3697 mgm^{-3} before the mucilage spread (Image 1) in the Dardanelles was calculated as 0.3728 mgm^{-3} at the time of the mucilage spread (Image 2). There was an increase of approximately 0.84%. In the Gulf of Izmit, the average chlorophyll-a concentration value, which was calculated as 0.684 mgm^{-3} before the mucilage spread (Image 3) started, was calculated as 0.7402 on May

Figure 6. Dardanelles Strait – Chlorophyll-a Concentration map (Left image before mucilage, right image after mucilage propagation).

Figure 7. Izmit Bay – Chlorophyll-a Concentration map (Left image before mucilage, right image after mucilage propagation).

Figure 8. Gemlik Bay – Chlorophyll-a Concentration map (Top image before mucilage, bottom image after mucilage propagation at ten days interval).

Table 4. Mean Chlorophyll-a Concentration values and changes for all study areas

Image Number	Mean Chlorophyll-a Concentration (mgm^{-3})	Mean Chlorophyll-a Concentration Change (%)
1	0,3697	–
2	0,3728	0,84
3	0,6840	–
4	0,7402	8,22
5	0,2372	–
6	0,8839	272,64
7	0,4366	84,06

19, 2021, the date of the mucilage spread (Image 4), with an increase of approximately 8.22%. Finally, the average chlorophyll-a concentration values in the Gulf of Gemlik were examined and it was calculated as 0.2372 mgm^{-3} before the mucilage spread (Image 5) began. Chlorophyll-a concentration values were obtained as 0.8839 mgm^{-3} and 0.4366 mgm^{-3}, respectively, on May 9 (Image 6), 2021 and May 19 (Image 7), 2021, when the mucilage areas in the region were the largest. When we look at the rate of increase in chlorophyll-a concentration in the Gulf of Gemlik, there has been a change of approximately 272.64% on the date when the most mucilage area was detected, compared to the date when mucilage did not begin to spread. On May 19, 2021, a change of approximately 84.06% was observed. Marine chlorophyll-a concentration maps obtained from satellite images are shown in Figure 6, Figure 7, and Figure 8.

The average chlorophyll-a concentration values calculated for all satellite images and their percentage changes are given in Table 4.

CONCLUSION

Within the scope of this study, mucilage, which is seen as the biggest ecological problem of the Marmara Sea in 2021, also called sea saliva, is discussed. Recently, remote sensing method as a rapidly evolving technology, provides the quick detection of mucilage so as to take early precaution for the mentioned environmental problem.

The selected regions within the scope of the study have strategic importance due to their location on maritime transport and trade routes. As a result of the analyzes and calculations, mucilage areas on the sea surface were determined quickly and were associated with the ratio of chlorophyll, an organic substance.

In this study, remote sensing methods were used to detect these organic substances. In addition, with the NDWI information used to determine the water areas, the mucilage collecting as a layer on the sea surface can be appropriately detected. It has been tried to show that the chlorophyll-a concentration is also high in images with increased mucilage areas. Chlorophyll-a concentration is not a parameter found in water only because of mucilage. Certain chlorophyll-a concentrations were detected in the study areas before the mucilage spread began. Different levels of chlorophyll-a concentration can be observed depending on different factors, independent of mucilage. But in the study aim in line with its purpose and the results, the increase in mucilage areas was associated with the increase in chlorophyll-a concentrations. It has also been shown in the study that when the mucilage areas and chlorophyll-a concentrations are compared visually, the mucilage spread can be accurately determined and suitable locations can be quickly determined to take precautions.

When inspecting the results, it was observed that the mucilage areas and the average chlorophyll-a concentration values in the satellite images taken before and after the event indicate a considerable correlation. This shows that remote

sensing provides the opportunity taking early precautions for mucilage, because of the rapid detection of the affected areas. In the future works, Dardanelles Strait to Black Sea will be examined within the disciplines of remote sensing and geographic information systems, and it is planned to work on risk analyzes on these routes.

AUTHORSHIP CONTRIBUTIONS

Authors equally contributed to this work.

DATA AVAILABILITY STATEMENT

The authors confirm that the data that supports the findings of this study are available within the article. Raw data that support the finding of this study are available from the corresponding author, upon reasonable request.

CONFLICT OF INTEREST

The author declared no potential conflicts of interest with respect to the research, authorship, and/or publication of this article.

ETHICS

There are no ethical issues with the publication of this manuscript.

REFERENCES

[1] United Nations. Sustainable Development Goals 2019. Available at: http://www.undp.org/content/undp/en/home/sustainable-development-goals.html (Accessed Sept 28, 2021).

[2] Türkiye İstatistik Kurumu 2021. Available at: https://www.tuik.gov.tr/ (Accessed Sept 28, 2021). [Turkish]

[3] Basar E. Oil spill simulations in the aftermath of tanker accident at the tanker routes in the Marmara Sea. International Oil Spill Conference. 2008:1215–1217. [CrossRef]

[4] Küçük YK, Topçu A. Deniz taşımacılığından kaynaklanan kirlilik. Ankara Üniversitesi Çevrebilimleri Dergisi 2012;4:75–80. [Turkish]

[5] Altuğ G, Çardak M, Çiftçi PS, Gürün S. First records and microgeographical variations of culturable heterotrophic bacteria in an inner sea (the Sea of Marmara) between the Mediterranean and the Black Sea, Turkey. Turk J Biol 2013;37:184–190. [CrossRef]

[6] Taşdemir Y. Marmara denizi: Kirleticiler ve çevre açısından alınabilecek tedbirler. Uludağ Üniversitesi Mühendislik-Mimarlık Fakültesi Dergisi 2002;7:39–45. [Turkish]

[7] Topcuoğlu S, Kirbaşoğlu Ç, Yilmaz YZ. Heavy Metal Levels in Biota and Sediments in the Northern Coast of the Marmara Sea. Environ Monitor Assess 2004;96:183–189. [CrossRef]

[8] Kut D, Topcuoğlu S, Esen N, Küçükcezzar R, Güven KC. Trace Metals in Marine Algae and Sediment Samples from the Bosphorus. Water Air Soil Pollut 2000;118:27–33. [CrossRef]

[9] Zingone A, Oksfeldt Enevoldsen H. The diversity of harmful algal blooms: a challenge for science and management. Ocean Coast Manag 2000;43:725–748. [CrossRef]

[10] Lancelot C, Spitz Y, Gypens N, Ruddick K, Becquevort S, Rousseau V, et al. Modelling diatom and Phaeocystis blooms and nutrient cycles in the Southern Bight of the North Sea: the MIRO model. Mar Ecol Progress Ser 2005;289:63–78. [CrossRef]

[11] Innamorati M, Nuccio C, Massi L, Mori G, Melley A. Mucilages and climatic changes in the Tyrrhenian Sea. Aquat Conserv 2001;11:289–298. [CrossRef]

[12] Mecozzi M, Acquistucci R, di Noto V, Pietrantonio E, Amici M, Cardarilli D. Characterization of mucilage aggregates in Adriatic and Tyrrhenian Sea: structure similarities between mucilage samples and the insoluble fractions of marine humic substance. Chemosphere 2001;44:709–720. [CrossRef]

[13] Precali R, Giani M, Marini M, Grilli F, Ferrari CR, Pečar O, et al. Mucilaginous aggregates in the northern Adriatic in the period 1999–2002: Typology and distribution. Sci Total Environ 2005;353:10–23. [CrossRef]

[14] Ciglenečki I, Plavšić M, Vojvodić V, Ćosović B, Pepi M, Baldi F. Mucopolysaccharide transformation by sulfide in diatom cultures and natural mucilage. Mar Ecol Progress Ser 2003;263:17–27. [CrossRef]

[15] Danovaro R, Umani SF, Pusceddu A. Climate change and the potential spreading of marine mucilage and microbial pathogens in the Mediterranean Sea. PLoS One 2009;4:e7006. [CrossRef]

[16] Degobbis D. Increased eutrophication of the northern Adriatic sea: Second act. Mar Pollut Bull 1989;20:452–457. [CrossRef]

[17] Calvo S, Barone R, Flores LN. Observations on mucus aggregates along Sicilian coasts during 1991–1992. Sci Total Environ 1995;165:23–31. [CrossRef]

[18] Tufekçi V, Balkis N, Polat Beken Ç, Ediger D, Mantikçi M. Phytoplankton composition and environmental conditions of a mucilage event in the Sea of Marmara. Turk J Biol 2010;34:199–210. [CrossRef]

[19] Artüz L. Marmara Denizi genelinde gözlemlenen karışık alg patlaması sonucunda oluşan musilaj agregat konusunda rapor 2008. Available at: https://docplayer.biz.tr/2054734-Marmara-denizi-genelinde-gozlemlenen-karisik-alg-patlamasi-sonucunda-olusan-musilaj-agregat-konusunda-rapor.html (Accessed on Sept 28, 2021). [Turkish]

[20] Keleş G, Yılmaz S, Zengin M. Possible economic effects of musilage on Sea of Marmara fisheries. Int J Agric Forestry Life Sci 2020;4:173–177.
[21] Zhao S, Wang Q, Li Y, Liu S, Wang Z, Zhu L, et al. An overview of satellite remote sensing technology used in China's environmental protection. Earth Sci Inform 2017;10:137–148. [CrossRef]
[22] Goldewijk KK. Estimating global land use change over the past 300 years: The HYDE Database. Global Biogeochemical Cycles 2001;15:417–433. [CrossRef]
[23] Moran E, Brondizio ES. Land-use change after deforestation in Amazonia. In: Liverman, D (editor). People and Pixels: Linking Remote Sensing and Social Science. Washington, D. C.: National Academy Press; 1998: 94–120.
[24] Polat AB, Akçay Ö. Rapid Flood Mapping with Sentinel-1 SAR Images: A Case Study of Maritsa River. 2nd Intercontinental Geoinformation Days (IGD), Mersin, Turkey: 2021, 123–126.
[25] Hafeez S, Sing Wong M, Abbas S, Kwok YT, Nichol J, Ho Lee K, et al. Detection and Monitoring of Marine Pollution Using Remote Sensing Technologies. Monitoring of Marine Pollution. London: IntechOpen; 2019. [CrossRef]
[26] Kolokoussis P, Karathanassi V. Oil spill detection and mapping using sentinel 2 imagery. J Mar Sci Eng 2018;6:4. [CrossRef]
[27] Naz S, Iqbal MF, Mahmood I, Allam M. Marine oil spill detection using Synthetic Aperture Radar over Indian Ocean. Mar Pollut Bull 2021;162:111921. [CrossRef]
[28] Majidi Nezhad M, Groppi D, Laneve G, Marzialetti P, Piras G. Oil Spill Detection Analyzing "Sentinel 2" Satellite Images: A Persian Gulf Case Study. World Congress on Civil, Structural, and Environmental Engineering 2018:8: AWSPT 134-1–AWSPT 134–8. [CrossRef]
[29] Misra A, Balaji R. Simple approaches to oil spill detection using sentinel application platform (SNAP)-ocean application tools and texture Analysis: A comparative study. J Indian Soc Remote Sens 2017;45:1065–1075. [CrossRef]
[30] Bukata R, Bruton J, Jerome J, Jain S, Zwick H. Optical water quality model of Lake Ontario. 2: Determination of chlorophyll a and suspended mineral concentrations of natural waters from submersible and low altitude optical sensors. Appl Optics 1981;20:1704. [CrossRef]
[31] Dekker AG, Brando VE, Anstee JM, Pinnel N, Kutser T, Hoogenboom EJ, et al. Imaging Spectrometry of Water. Dordrecht: Springer; 2002. [CrossRef]
[32] Koponen S, Pulliainen J, Kallio K, Hallikainen M. Lake water quality classification with airborne hyperspectral spectrometer and simulated MERIS data. Remote Sens Environ 2002;79:51–59. [CrossRef]
[33] Cui TW, Zhang J, Wang K, Wei JW, Mu B, Ma Y, et al. Remote sensing of chlorophyll a concentration in turbid coastal waters based on a global optical water classification system. ISPRS J Photogrammetry Remote Sens 2020;163:187–201. [CrossRef]
[34] Acar U, Yilmaz OS, Çelen M, Ateş AM, Gülgen F, Balık Şanlı F. Determination of mucilage in the sea of Marmara using remote sensing techniques with Google Earth engine. Int J Enivron Geoinform 2021;8:423–434. [CrossRef]
[35] Kavzoğlu T, Tonbul H, Çölkesen İ, Sefercik UG. The use of object-based image analysis for monitoring 2021 marine mucilage bloom in the Sea of Marmara. Int J Environ Geoinform 2021;8:529–536. [CrossRef]
[36] Platt T, Sathyendranath S. Ecological indicators for the pelagic zone of the ocean from remote sensing. Remote Sens Environ 2008;112:3426–3436. [CrossRef]
[37] Huang C, Zou J, Li Y, Yang H, Shi K, Li J, et al. Assessment of NIR-red algorithms for observation of chlorophyll-a in highly turbid inland waters in China. ISPRS J Photogrammetry Remote Sens 2014;93:29–39. [CrossRef]
[38] Ansper A, Alikas K. Retrieval of chlorophyll a from sentinel-2 MSI data for the european union water framework directive reporting purposes. Remote Sens 2018;11:64. [CrossRef]
[39] Zhang Y, Ma R, Duan H, Loiselle S, Xu J. A Spectral Decomposition Algorithm for Estimating Chlorophyll-a Concentrations in Lake Taihu, China. Remote Sens 2014;6.:5090–5106. [CrossRef]
[40] Woźniak M, Bradtke KM, Krężel A. Comparison of satellite chlorophyll a algorithms for the Baltic Sea. J Appl Remote Sens 2014;8:083605. [CrossRef]
[41] Kavurmacı M, Ekercin S, Altaş L, Kurmaç Y. Use of EO-1 Advanced Land Imager (ALI) multispectral image data and real-time field sampling for water quality mapping in the Hirfanlı Dam Lake, Turkey. Environ Sci Pollut Res 2013;20:5416–5424. [CrossRef]
[42] Watanabe FSY, Alcântara E, Rodrigues TWP, Imai NN, Barbosa CCF, Rotta LH da S. Estimation of chlorophyll-a concentration and the trophic state of the barra bonita hydroelectric reservoir using OLI/landsat-8 Images. Int J Environ Res Public Health 2015;12:10391–10417. [CrossRef]
[43] Augusto-Silva PB, Ogashawara I, Barbosa CCF, Carvalho LAS de, Jorge DSF, Fornari CI, et al. Analysis of MERIS reflectance algorithms for estimating chlorophyll-a Concentration in a Brazilian Reservoir. Remote Sens 2014;6:11689–1707. [CrossRef]
[44] Toming K, Kutser T, Laas A, Sepp M, Paavel B, Nõges T. First experiences in mapping lake water quality parameters with sentinel-2 MSI imagery. Remote Sens 2016;8:640. [CrossRef]
[45] Du Y, Zhang Y, Ling F, Wang Q, Li W, Li X. Water bodies' mapping from sentinel-2 imagery with

modified normalized difference water index at 10-m spatial resolution produced by sharpening the SWIR band. Remote Sens 2016;8:354. [CrossRef]

[46] European Space Agency. Sentinel Online - ESA - Sentinel Available at: https://sentinel.esa.int/web/sentinel/home (Accessed Sept 28, 2021).

[47] Vanhellmont Q, Ruddick K. Acolite for Sentinel-2: Aquatic Applications of MSI Imagery. ESA Living Planet Symposium 2016;740:55.

[48] McFeeters SK. The use of the Normalized Difference Water Index (NDWI) in the delineation of open water features. Int J Remote Sens 1996;17:1425–1432. [CrossRef]

[49] Aksoy T, Sarı S, Çabuk A. Sulak alanların yönetimi kapsamında su indeksinin uzaktan algılama ile tespiti, göller yöresi. GSI J B Adv Bus Econ 2019;2:35–48. [Turkish]

[50] Talukdar S, Pal S. Effects of damming on the hydrological regime of Punarbhaba river basin wetlands. Ecol Eng 2019;135:61–74. [CrossRef]

[51] Xu H. Modification of normalised difference water index (NDWI) to enhance open water features in remotely sensed imagery. Int J Remote Sens 2006;27:3025–3033. [CrossRef]

[52] Türkiye Cumhuriyeti Çevre ve Şehircilik Bakanlığı. Çevresel Göstergeler, Kıyı ve Deniz Sularında Klorofil-a Miktarı 2018. Available at: https://cevre-selgostergeler.csb.gov.tr/kiyi-ve-deniz-sularinda-klorofil-a-miktari-i-85743 (Accessed on Sept 28, 2021). [Turkish]

[53] Ritchie JC, Zimba P. Everitt JH. Remote sensing techniques to assess water quality. Photogrammetric Eng Remote Sens 2003;69:695–704. [CrossRef]

[54] Gitelson A. The peak near 700 nm on radiance spectra of algae and water: relationships of its magnitude and position with chlorophyll concentration. Int J Remote Sens 1992;13:3367–373. [CrossRef]

[55] Gitelson AA, Gurlin D, Moses WJ, Barrow T. A bio-optical algorithm for the remote estimation of the chlorophyll-a concentration in case 2 waters. Environ Res Lett 2009;4:045003. [CrossRef]